Photoluminescence excitation spectra of lanthanide doped YAlO$_3$ in vacuum ultraviolet region

Yuhei Shimizu [a], Kazushige Ueda [a, *], Yoshiyuki Inaguma [b]

[a] Department of Materials Science, Graduate School of Engineering, Kyushu Institute of Technology, 1-1 Sensui, Tobata, Kitakyushu 804-8550, Japan
[b] Department of Chemistry, Faculty of Science, Gakushuin University, 1-5-1 Mejiro, Toshima-ku, Tokyo 171-8588, Japan

ARTICLE INFO

ABSTRACT

To understand luminescent mechanisms of lanthanide (Ln) doped phosphors, it is important to know the energy positions of unoccupied Ln^{2+} 4f and Ln^{3+} 5d states, as well as occupied Ln^{3+} 4f states, relative to the energy bands of host materials. Photoluminescence excitation (PLE) spectra of Ln doped YAlO$_3$ were measured in a vacuum ultraviolet (VUV) region and the energy positions of Ln^{2+} 4f and Ln^{3+} 5d states in the wide-gap YAlO$_3$ were elucidated. Peaks assignable to host lattice excitation were observed in all samples at approximately 8 eV in the PLE spectra. PLE peaks derived from charge transfer (CT) and 4f-5d transitions were observed at lower energy than the bandgap energy. Ln^{2+} 4f energy levels were obtained from the PLE peak energies for the CT transitions along with the valence band maximum. In contrast, Ln^{3+} 5d energy levels were evaluated from those for the 4f-5d transitions along with the Ln^{3+} 4f energy levels, which were obtained previously from X-ray photoelectron spectroscopy measurements. The elucidated Ln^{2+} 4f and Ln^{3+} 5d energy levels were exhibited in an energy diagram together with Ln^{3+} 4f energy levels and host energy bands. The experimental Ln^{2+} 4f and Ln^{3+} 5d energy levels were in good agreement with the reported theoretical data.

© 2017 Elsevier B.V. All rights reserved.

1. Introduction

Various perovskite-type oxide phosphors doped with trivalent lanthanide ions (Ln^{3+}) have been developed lately and their luminescent properties have been investigated [1–5] even though the properties of some phosphors such as BaTiO$_3$:Sm^{3+} were reported several decades ago [6]. The developed phosphors show not only visible luminescence but also infrared or ultraviolet luminescence to be used in their diverse application. Many luminescent centers are used for visible luminescent phosphors and especially Eu^{3+}, Tb^{3+}, and Tm^{3+} are well-known as RGB luminescent centers [7–11]. Nd^{3+} and Yb^{3+} are frequently used for luminescent centers of infrared phosphors [12–15] and Ce^{3+}, Pr^{3+}, and Gd^{3+} are for ultraviolet (UV) phosphors [16–18]. The wavelengths of the luminescence sometimes confine chemical compositions of host materials, especially in UV luminescence. Wide gap materials such as YAlO$_3$, LuAlO$_3$, and YScO$_3$ are employed for host materials of ultraviolet phosphors due to their high energy luminescence [19–21].

The perovskite-type oxide phosphors are promising materials for thin film-type luminescent devices, because they have high chemical stability and their high quality epitaxial thin films frequently grow on perovskite single crystal substrates [22–25]. Actually, electroluminescence (EL) devices using perovskite-type oxide phosphor thin films were fabricated [26–28] and an EL device using (Ca$_{0.6}$Sr$_{0.4}$)TiO$_3$:Pr^{3+} for luminescent layers were reported to show high luminance above one hundred cd/m^2 [28]. Accordingly, further development of new materials and their application are anticipated in perovskite-type oxide phosphors.

Simultaneously with the materials development and device application, investigations of luminescence mechanisms are also important in Ln doped phosphors. For understanding the luminescence mechanisms, it will be essential to clarify energy levels of luminescent centers in host energy bands. Multiplet excited 4f energy levels relative to the 4f ground level in each Ln^{3+} ion are hardly influenced by host materials as widely known in Dieke diagram [29]. Relative 4f ground energies among Ln^{3+} ions, namely zigzag energy curves, are also almost independent of host materials [30]. However, relative energies between the Ln^{3+} 4f ground levels and host energy bands are dependent on host materials [31,32]. It was recently reported that the values of the Ln energy levels

relative to host energy bands or the vacuum level are able to be determined from not only a large number of referential data but also theoretical considerations [33,34]. Accordingly, the energy diagrams of Ln energy levels were successfully drawn in many compounds [35–37] and these diagrams will help us to develop new phosphors as well as to understand luminescence mechanisms.

In our recent studies on the development of UV phosphors and UV emissive devices, not only the UV luminescence properties of Gd^{3+} doped $YAlO_3$ perovskite-type phosphors [18,25] but also the Ln^{3+} $4f$ energies in $YAlO_3$ were examined experimentally. The Ln^{3+} $4f$ ground energy levels in Ln^{3+} doped $YAlO_3$ were determined by X-ray photoelectron spectroscopy [38,39]. However, unoccupied Ln^{2+} $4f$ and Ln^{3+} $5d$ energies in Ln doped $YAlO_3$ have not been sufficiently examined yet. Accordingly, photoluminescence excitation (PLE) spectra in a vacuum ultraviolet (VUV) region were measured using synchrotron radiation in this study. Peaks in the PLE spectra were analyzed and consequently Ln^{2+} $4f$ and Ln^{3+} $5d$ energies in $YAlO_3$ were elucidated experimentally.

2. Experiments

Ln^{3+} (1 at%)-doped $YAlO_3$ samples (Ln = Ce, Pr, Nd, Eu, Gd, Tb, and Tm) were prepared by a polymerized complex method [40] to mix starting materials homogeneously. Y_2O_3 (99.99%), $Al(NO_3)_3 \cdot 9H_2O$ (99.9%), $Ce(NO_3)_3 \cdot 6H_2O$ (99.9%), Pr_6O_{11} (99.9%), Nd_2O_3 (99.9%), Eu_2O_3 (99.9%), Gd_2O_3 (99.9%), Tb_4O_7 (99.9%), Tm_2O_3 (99.9%), and Lu_2O_3 (99.9%) were used as the starting materials. The starting materials were dissolved in nitric acid. Propylene glycol and citric acid ethanol solution were added to the starting material solution, and the solution was stirred. Molar ratio of total cations in the starting materials and citric acid was set to be 1:5. The solution was heated and stirred at 80 °C for 2 h for complex formation, and then further heated and stirred at 150 °C for 4 h for polymerization. With the formation of polymerized complexes, the color of the solution changed gradually from colorless to dark brown and its viscosity increased. Soot-like precursors were obtained by heating the solution at 350 °C for 3 h. Powder samples were prepared by calcining the precursors at 1400 °C for 6 h in air. Ceramic samples with low density (approximately 70%) for PLE measurements were obtained by pressing the powder samples into φ 10 mm disks and sintering them at 1400 °C for 6 h in air. Since the samples were porous, their surfaces were rough like pressed powder samples.

PL spectra in UV and visible regions and PLE spectra in VUV and UV regions were measured in the wavelength range from 300 to 640 nm, and from 120 to 300 nm, respectively. The measurements were carried out at the BL3B beamline of UVSOR facility in Institute for Molecular Science. The BL3B beamline, which consists of a 2.5 m off-plane eagle-type normal-incidence monochromator with three-type spherical gratings, provided an incident light in a wide VUV to visible range. PL under VUV excitation were monitored by a monochromator (Acton Research Corporation, SpectraPro-300i) with a CCD detector for PL spectra and a photomultiplier for PLE spectra through an optical fiber [41]. PL and PLE spectra in a UV region of Ce doped sample were measured using a conventional spectrofluorometer (Jasco, FP-6500) with Xe lamp.

3. Results and discussion

Fig. 1(a) and (b) shows PL and PLE spectra of some Ln^{3+} doped $YAlO_3$ samples (Ln = Nd, Eu, Gd, Tm). The PL spectra in Fig. 1(a) measured under VUV excitation at 157 nm show typical sharp PL peaks originating from the doped Ln^{3+} ions. The peaks were assignable to $4f$-$4f$ transitions in each Ln^{3+} ion and the assignments of some typical peaks are indexed in Fig. 1(a) [30,42–46].
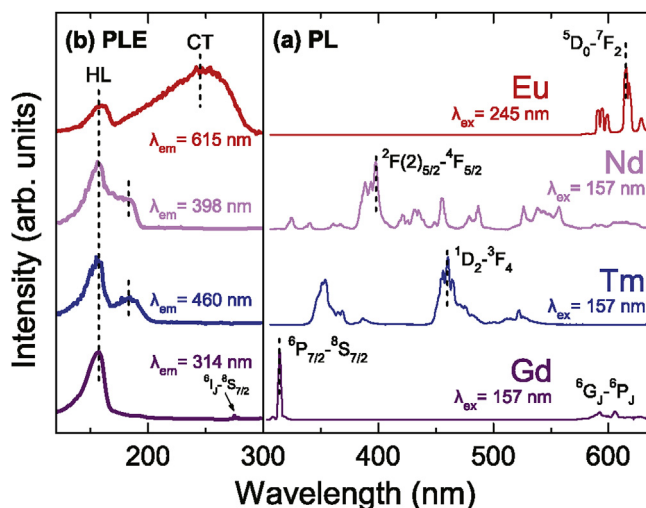

Fig. 1. (a) PL and (b) PLE spectra of Ln^{3+} doped $YAlO_3$ (Ln = Nd, Eu, Gd, Tm). λ_{ex} and λ_{em} show excitation wavelength for PL and monitored emission wavelength for PLE, respectively. Marks of dashed lines indicate typical emission and excitation peaks. CT and HL peaks in PLE spectra were attributed to charge transfer transition and host lattice excitation, respectively.

Monitoring the most intense PL peaks for the Ln^{3+} ions, PLE spectra were measured. In Fig. 1(b), common PLE peaks were observed at 157 nm (7.9 eV) in all the samples. Because the band gap energy of $YAlO_3$ is approximately 8 eV [47], the peaks at 157 nm were attributed to host lattice (HL) excitation. In HL excited PL, electrons in the valence band (VB) were excited to the conduction band (CB) and the excitation energy was transferred to doped Ln^{3+} ions resulting in the $4f$-$4f$ transitions within them (Fig. 2). In a Gd^{3+} doped sample, no strong PLE peaks were observed except for HL excitation although weak sharp PLE peaks of the $4f$-$4f$ transitions (^8S_J-^6I_J) at 277 nm were slightly observed. In other samples, strong broad peaks were observed in long wavelength sides of HL excitation peaks. Judging from the broad shape, the peaks were attributed to charge transfer (CT) or $4f$-$5d$ transitions (Fig. 2). Eu^{3+} ions have been investigated extensively as red emission centers in many materials [30]. The broad PLE band observed in the Eu^{3+} doped sample can be seen in ordinary UV region as frequently observed in many Eu^{3+} doped materials and the origin of the peak is widely recognized to be due to the CT transitions [48]. Therefore, the peak observed at 245 nm (5.1 eV) in the Eu^{3+} doped $YAlO_3$ is simply attributed to the CT transitions. In both Nd^{3+} doped and Tm^{3+} doped $YAlO_3$, broad peaks were observed at 183 nm (6.8 eV). The assignment of these peaks is not as easy as the Eu^{3+} doped sample, because there are few reports on PLE spectra for Nd^{3+} and Tm^{3+} ions in a VUV region.

The assignments of the broad PLE peaks in the Nd^{3+} doped and Tm^{3+} doped samples were attempted by utilizing an energy diagram of $YAlO_3$:Ln as shown in Fig. 3. Prior to the peak assignments, the energy diagram of Fig. 3 was drawn in the following procedures on the basis of experimental data of XPS spectra, optical absorption, and theoretical data in several references [36–39,47].

Firstly, host band energies, namely a CB minimum (CBM) and a VB maximum (VBM), were drawn with the bandgap energy of 8.0 eV from the optical absorption [47], setting the energy of the VBM to 0.0 eV in an energy axis. Secondly, the energies of Ln^{3+} $4f$ ground states, which have been already determined by XPS measurements in previous study [38,39], were plotted as circle symbols. Closed circle symbols show experimental data in the XPS measurements and open circle symbols show zigzag relative energies among Ln^{3+} ions, $\Delta E(n,6,3+)$ [36], fitting to the experimental closed